A Random Sequential Adsorption Model for Protein Adsorption to Surfaces Functionalized with Poly(ethylene oxide)

By *Parag Katira*, *Ashutosh Agarwal*, and *Henry Hess**

Surfaces that are designed to prevent the adsorption of proteins are of paramount importance in biomaterials science and engineering, and significant effort has been made to understand the factors contributing to the non-fouling properties of a wide variety of surface coatings. A particularly successful and common design strategy is the functionalization of the surface with poly(ethylene oxide) (PEO) at a range of molecular weights and grafting densities. We present a random sequential adsorption (RSA) model which focuses on the random distribution of polymer chains on the surface leading to polymer-free ''bald'' spots. The calculated density of such spots with a defined minimum diameter matches the experimentally determined adsorption density of proteins for different grafting densities and chain lengths. While the calculation relies on drastic simplifications of this complex problem, the results suggest that the random arrangement of polymer chains is a critical factor in primary protein adsorption to polymer-functionalized surfaces.

Theoretical attempts at understanding the effect of PEO-grafted polymers on the adsorption of proteins to surfaces have a long history.[1–3] Starting with Jeon et al.'s work based on de Gennes' theory of polymer brushes,[4,5] followed by the single chain mean field (SCMF) theory elaborated by Szleifer et al.,[6,7] to molecular dynamics simulations by Latour et al.[8] and Jiang et al.,[9] an increasingly detailed picture of the thermodynamics and kinetics of the adsorption process has been assembled. Theoretical results can be compared to experimental datasets, which measure adsorption for different proteins, polymer lengths, and grafting densities.[10,11]

Common to all previous theories and simulations is that the polymer chains are evenly distributed across the surface, with a constant spacing determined by the grafting density (Fig. 1A). However, the distribution of the polymer chains is close to random for three reasons (Fig. 1B): (i) the density of potential polymer attachment sites on the surface is significantly larger (e.g., 15 nm^{-2} for a gold surface[12]) than the grafting density of the polymer chains (ranging from 0.1 to 5 chains nm^{-2}),[13] (ii) the polymer chains interact with each other only at high grafting densities, and (iii) the covalent attachment of the chains precludes a reordering of the polymer distribution after the initial attachment. A random distribution of polymer chains leads to stochastically distributed protein binding sites defined by the absence of polymer chains. In contrast to previous theories focusing on the interactions between protein, polymer, and solvent, our hypothesis is that the existence of such ''bald spots'' is the primary cause of residual protein adsorption to PEO-grafted surfaces.

To test this hypothesis, a RSA model is developed which aims to (i) predict protein adsorption based on a small number of readily accessible parameters inserted into a single equation, and (ii) emphasize the stochastic placement of the grafted polymer chains on the surface (as opposed to a regular placement of grafting sites[7]) while neglecting every detail of the interaction of the polymer chains with solvent, surface, protein, and other chains. RSA models can be applied to a wide range of situations if the adsorption is irreversible on experimental timescales and an adsorbed particle blocks a further adsorption at that site.[14] Both conditions are met in the case of protein adsorption.[15]

We extend previous RSA models of protein adsorption to bare surfaces[16] by modeling the grafted polymers as randomly distributed, preexisting obstacles on the surface (Fig. 1C). For simplicity, the space occupied by the polymer chain is modeled as spherical with a radius equal to the radius of gyration of the polymer chain. The polymer chain excludes proteins (also assumed to be spherical[5,17,18]) from this sphere, but allows partial overlap by other polymer chains up to the experimentally determined maximal grafting density (Fig. 1C). Under these assumptions, we (i) calculate the open surface area required for the protein to reach the surface, (ii) determine the probability that a protein encounters an open spot of sufficient size, (iii) calculate the adsorption kinetics, and (iv) model secondary adsorption to PEO-chains terminated with hydrophobic groups.

(i) The contact between protein and surface requires a circular opening in the polymer layer with a minimum area of $A_{poly} = 2\pi d_p R_g$, where d_p is the protein diameter and R_g is the radius of gyration of the grafted polymer (see Figure 1 for geometry). The radius of gyration is calculated according to $R_g^2 = nbl_k\cos(\psi)/6$ for $n > 12$ and $R_g^2 = nb^2/6$ for smaller chains. Here, $l_k = 1$ nm is the Kuhn length of the polymer, n is the degree of polymerization,

[*] Prof. H. Hess, P. Katira, A. Agarwal
Department of Materials Science and Engineering,
University of Florida
Gainesville, Fl 32611-6400 (USA)
E-mail: hhess@mse.ufl.edu

DOI: 10.1002/adma.200802057

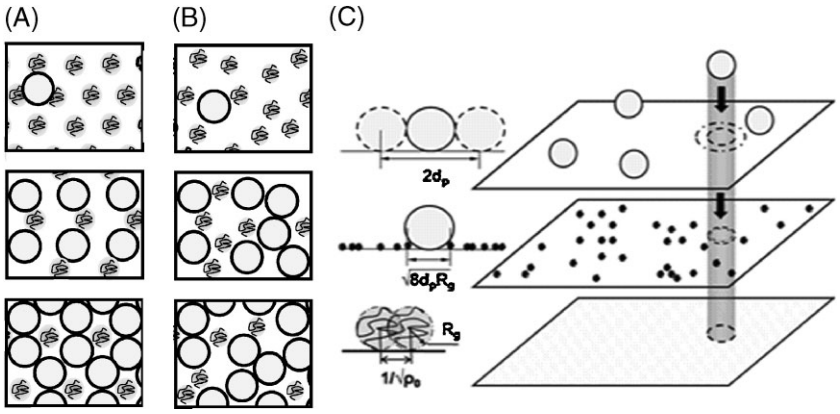

Figure 1. Concept of the random sequential adsorption model. A) In previous models, polymer chains are regularly distributed on the surface and the calculation focuses on determining the fluctuating shape of the polymer and its interaction with adsorbing proteins. As the grafting density increases, the polymer chains create a thermodynamic and kinetic barrier to adsorption, which proteins can overcome over time. B) In the random sequential adsorption model (RSA) polymer chains are randomly distributed and treated as hard spheres obstructing protein adsorption. As the grafting density increases, the number of unobstructed areas of sufficient size for protein adsorption decreases rapidly. C) A protein diffusing in solution has to encounter an adsorption site on the surface which is free of grafted polymers as well as already adsorbed proteins in order to irreversibly adsorb to the surface.

$b = 0.278$ nm is the monomer length and $\psi = 37.5^\circ$ is the angle between the chain axis and the bond between monomers.[19] Similarly, proteins already adsorbed within an area $A_{\text{prot}} = \pi {d_p}^2$ will obstruct contact between the adsorbing protein and the surface.

(ii) The number of polymer chains within a surface area A is randomly distributed with a mean $\mu = \rho A$ where ρ is the surface density of polymer chains (number per area). At the maximum grafting density ρ_0 the maximum number of polymer chains within the surface area A is either $floor(\rho_0 A)$ or $ceil(\rho_0 A)$, where $floor(N)$ is the greatest integer value less than N and $ceil(N)$ is the smallest integer value greater than N. Thus, for each encounter of the protein with the surface, there are either $floor(\rho_0 A)$ or $ceil(\rho_0 A)$ separate locations for a polymer chain within the area, and each of these locations is occupied with a probability of $x = \rho/\rho_0$ (the grafting ratio). The number of polymers in each area A is therefore given by two binomial distributions with the same probability of success x but two different number of trials. Since the average maximum number of polymers chains within area A is given by $\rho_0 A$, the binomial distribution with $floor(\rho_0 A)$ trials has to be invoked in the fraction $ceil(\rho_0 A) - \rho_0 A$ of all collisions, and the binomial distribution with $ceil(\rho_0 A)$ trials has to be invoked in the fraction $\rho_0 A - floor(\rho_0 A)$ of all protein–surface collisions.

The probability that there are zero polymers in the area A_{poly} is given by

$$P_{poly}(0) = (\text{ceil}(\rho_0 A_{poly}) - \rho_0 A_{poly})^* (1-x)^{floor(\rho_0 A_{poly})} + (\rho_0 A_{poly} - \text{floor}(\rho_0 A_{poly}))^* (1-x)^{ceil(\rho_0 A_{poly})} \quad (1)$$

which can be approximated by

$$P_{poly}(0) = (1-x)^{\rho_0 A_{poly}} \quad (2)$$

as shown in the Supporting Information, Figure S1A. Therefore, the probability that a protein scanning the surface encounters an opening of the required size in the polymer layer is approximated by Equation 2.

If σ is the density of adsorbed proteins on the surface, then the actual density of proteins within the area of the surface not covered by the polymers is $\sigma/(1-x)$. We model the distribution of already adsorbed proteins in the interaction area A_{prot} also as two binomial distributions with mean $\mu = A_{\text{prot}}\sigma/(1-x)$ and number of trials $floor(A_{\text{prot}}\ \sigma_0)$ and $ceil(A_{\text{prot}}\ \sigma_0)$, respectively with $\sigma_0 = 4f/\pi {d_p}^2$ as the maximum theoretical protein density. Utilizing the same approximation described above, the probability that there is no adsorbed protein obstructing the interaction of an incoming protein and the surface is then given by

$$P_{prot}(0) = \left(1 - \frac{\sigma}{\sigma_0(1-x)}\right)^{\sigma_0 A_{prot}} = \left(1 - \frac{\sigma}{\sigma_0(1-x)}\right)^{4f} \quad (3)$$

Here we take $f = 0.9$ for hexagonal closed packing of proteins on the surface.

We use the approximated probability distributions for polymers as well as adsorbed proteins for all further calculations for the sake of mathematical simplicity. It is shown in the Supporting Information, Figure S1B and C, that this approximation has no discernible effect on the predicted protein adsorption values.

(iii) The rate of collisions between proteins and surface per unit area Z is given by[20,21] $Z = C_p\sqrt{k_b T/m_p}$, where C_p is the protein concentration and m_p is the mass of the protein. The probability that a collision with the bare surface results in adsorption is denoted by the sticking probability S and has values ranging from 10^{-5} to 10^{-8} for typical proteins and surfaces.[20]

The rate of protein adsorption on the surface grafted with polymers is then given by

$$\frac{d\sigma}{dt} = ZS^* P_{poly}(0)^* P_{prot}(0) \quad (4)$$

Solving this differential equation yields:

$$\sigma = \frac{4f(1-x)}{\pi d_p^2}\left\{1 - \left[1 + \frac{\pi d_p^2 (4f-1) SZt}{4f(1-x)}(1-x)^{2\rho_0 \pi d_p R_g}\right]^{-1/(4f-1)}\right\} \quad (5)$$

(iv) In cases where the terminal group on the hydrophilic polymer is a hydrophobic group such as OCH_3 instead of OH, high grafting coverage shows increased protein adsorption.[13] This can be the result of secondary protein adsorption to a close-packed layer of hydrophobic groups on top of the hydrophilic chains. Assuming that the smallest polymer island creating such secondary adsorption sites requires six close-packed polymer chains,[18] the probability of a protein encountering a secondary adsorption site is given by $P_{isl}(6) = x^6$. In this case, the probability $P_{prot}(0)$ of a protein-surface contact unobstructed by already adsorbed proteins can be approximated by

$$P_{prot}(0) = (1 - \sigma/\sigma_0)^{\sigma_0 A_{prot}} = (1 - \sigma/\sigma_0)^{4f} \quad (6)$$

since the proteins are adsorbed on top of and between polymer islands. If different sticking probabilities exist for adsorption to the bare surface and to top of the polymer islands, denoted by S and S_{isl}, the combined rate of protein adsorption to a primary or secondary adsorption site is given by:

$$\frac{d\sigma}{dt} = Z^*[SP_{poly}(0) + S_{isl}P_{isl}(6)]^* P_{prot}(0) \quad (7)$$

Solving for σ yields:

$$\sigma = \frac{4f}{\pi d_p^2}\left\{1 - \left[1 + \frac{\pi d_p^2(4f-1)Zt}{4f}(S(1-x)^{2\rho_0 \pi d_p R_g} + S_{isl}x^6)\right]^{-1/(4f-1)}\right\} \quad (8)$$

which reflects the dominant contribution of primary adsorption sites at low grafting densities, and the increasing contribution of secondary adsorption at high grafting densities.

Due to the small number of parameters, the predictions of the above model can be directly compared to published experimental results. Here we focus on three studies[11,13,22] to illustrate the excellent agreement between theory and experiment.

Prime and Whitesides mapped the adsorption of fibrinogen, pyruvate kinase, lysozyme and ribonuclease A as a function of ethylene oxide chain length ($n = 0$–17) and fraction of oligo(ethylene oxide)-terminated alkanethiols in a self-assembled monolayer.[11] Figure 2 shows the experimental data and theoretical predictions for ribonuclease A. The size of the ribonuclease A protein d_p is taken as 3.8 nm and the molecular weight as 12.7 kDa.[23,24] The maximum possible

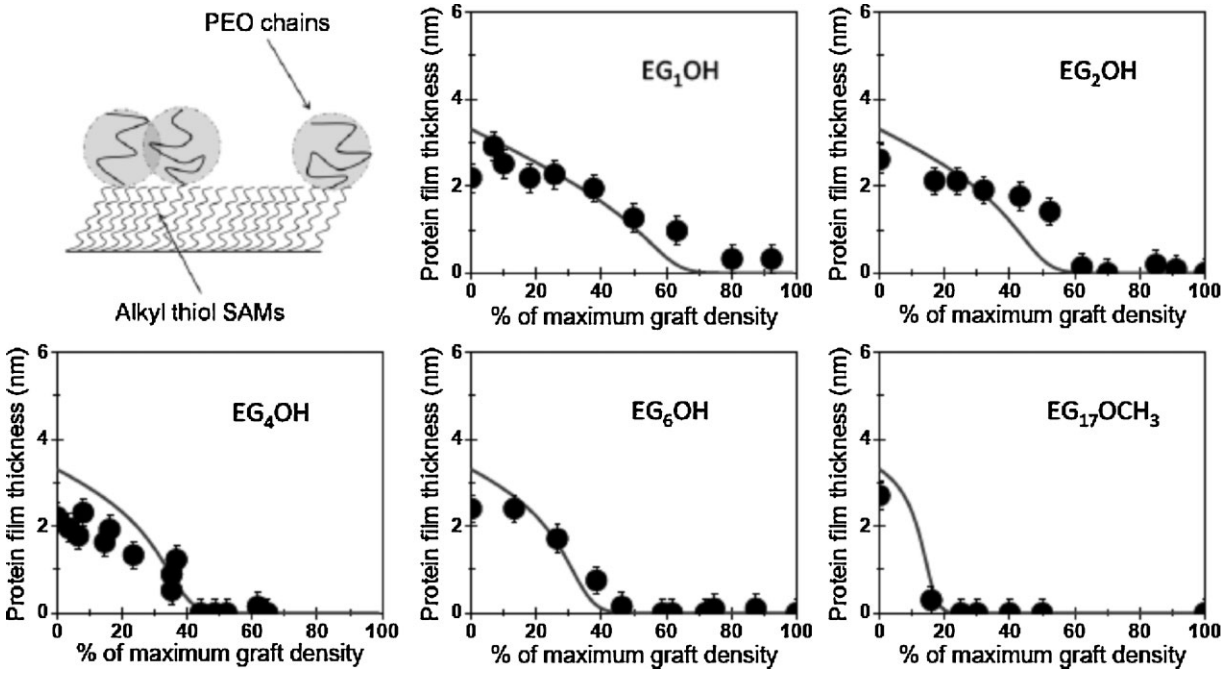

Figure 2. Comparison with experimental data of Prime et al. [11]. The adsorption of ribonuclease A to PEO-grafted SAM surfaces as a function of polymer graft coverage as experimentally observed (black circles) and as predicted by the RSA model (solid line). The maximum graft density is 4.07, 3.93, 3.6, 3.46, and 2.42 nm^{-2} for EGOH, EG_2OH, EG_4OH, EG_6OH, and $EG_{17}OCH_3$, respectively.

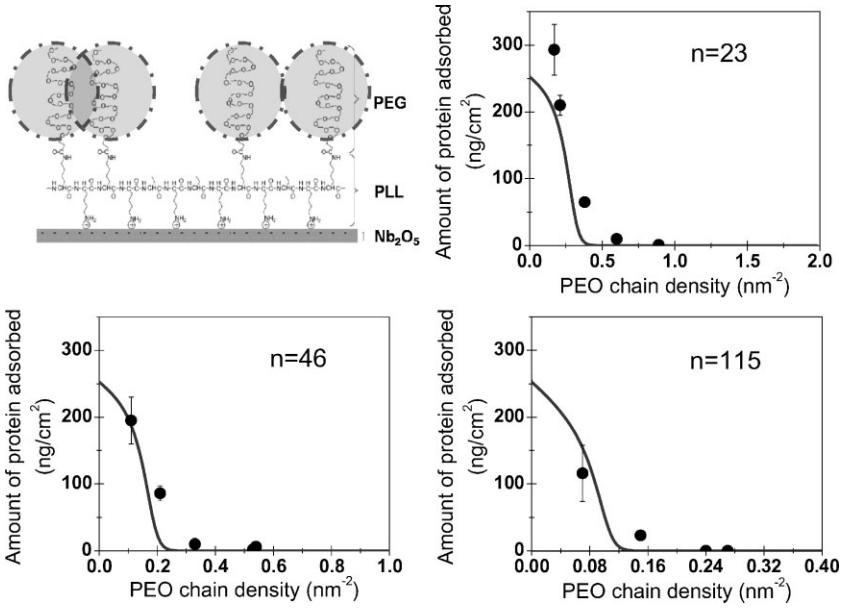

Figure 3. Comparison with experimental data of Pasche et al. [22]. The adsorption of serum protein to PEG-grafted surfaces as function of PEO chain density as experimentally observed (black circles) and as predicted by the RSA model (solid line).

graft density ρ_0 is chosen based on experimental data when available[13,25] and interpolations of the experimental data as described in Supplementary Information, Figure S2. Secondary adsorption is not observed for methyl-terminated PEO chains ($n = 17$), presumably due to the rinsing step prior to measurement. The value of Zt is calculated from the protein concentration (1 mg mL^{-1}) and the adsorption time (120 min) utilized in the experiment, while S is chosen as 8.8×10^{-8} according to measurements by Weaver et al. for the adsorption of albumin to silica.[20] The value of SZt does not greatly influence the predicted protein adsorption, thus an approximation of the actual value is sufficient (Fig. 5D). A comparison between the RSA model and experimental data for lysozyme can be found in the Supporting Information, Figure S3. The experimental data for pyruvate kinase and fibrinogen–proteins with a cylindrical rather than spherical shape–have not been fitted with the basic model presented here.

Pasche et al.[22] provide data for the adsorption of serum to PLL-g-PEG-coated Nb_2O_5 surfaces for PEG chains with molecular weights of 1, 2, and 5 kDa ($n = 23$, 46 and 115) and varying grafting ratios (Fig. 3). Serum (~85 mg mL^{-1} protein concentration) was adsorbed for 15 min. Since albumin constitutes a majority of serum proteins, the protein diameter is chosen as 7 nm,[26] and the adsorbed protein number density is calculated from the adsorbed mass using a molecular weight of 66 kDa. The value of the sticking probability S is again assumed to be 8.8×10^{-8}. The maximum graft density for the different PEG lengths was interpolated from experimental data of maximum PEO graft densities as function of length in the literature (see the Supporting Information, Fig. S2).[13,25]

Unsworth et al.[13] measure protein adsorption to surfaces coated with hydroxyl-terminated (600 Da) and methyl-terminated (750 Da, 2000 Da) thiolated PEO chains as well as the transient and maximal (4 h incubation) grafting density (Fig. 4). Lysozyme ($d_p = 4.5$ nm, $M_w = 14$ kDa[27]) is adsorbed for 180 min at a concentration of 1 mg mL^{-1}. Methyl-terminated PEO-coated surfaces display secondary adsorption as the grafting ratio is increased, and consequently Equation 8 is utilized. For primary adsorption to the surface coated with hydroxyl-terminated PEO chains we again assume a value of the sticking probability S of 8.8×10^{-8} (Fig. 4, left). For secondary adsorption onto islands of methyl-terminated PEO grafts, the sticking probability is not known and the predictions of the RSA model are displayed for our standard sticking probability of 8.8×10^{-8} as well as for a two hundred-fold smaller sticking probability for 750 Da PEO chains and two thousand-fold smaller sticking probability for 2000 Da PEO chains (Fig. 4, right).

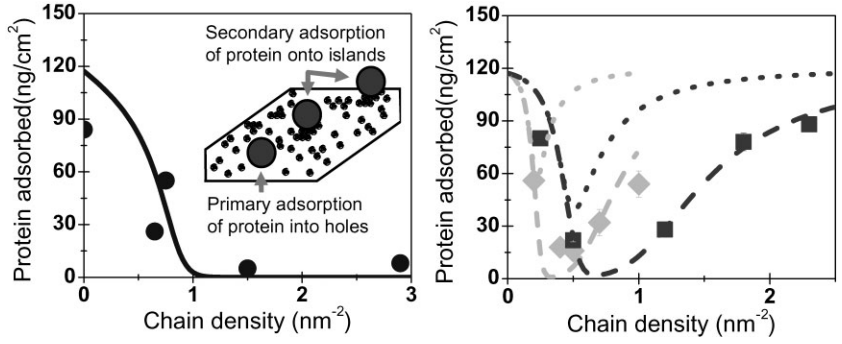

Figure 4. Comparison with experimental data of Unsworth et al. [13]. Left: Primary adsorption to surfaces grafted with hydroxyl-terminated PEO chains ($M_w = 600$ Da) as experimentally observed (black circles) and as predicted by Equation 5 (solid line). Right: Primary and secondary adsorption to surfaces grafted with methyl-terminated PEO for $M_w = 750$ Da (squares) and $M_w = 2000$ Da (diamonds) as experimentally observed and predicted by Equation 8. Dotted lines represent a sticking probability of 8.8×10^{-8} for both, primary and secondary adsorption sites. Dashed lines represent a sticking probability of 8.8×10^{-8} for primary adsorption and a lower sticking probability for secondary adsorption (4.4×10^{-10} for 750 Da, black, and 4.4×10^{-11} for 2000 Da, gray.).

The correspondence between the experimental data and the theoretical predictions despite the complete neglect of any thermodynamic and structural detail is striking. The calculation utilizes the protein diameter, concentration, time of exposure, and sticking probability, as well as the polymer chain density, chain length, and maximal chain density to reproduce the non-trivial dependence of protein adsorption on polymer chain density and chain length observed in experiments by three different research groups for three different systems (PEO-terminated alkanethiol SAMs, physisorbed PEO-grafted poly(L-lysine), end-thiolated PEO chemisorbed

to gold). This indicates that the model is robust, meaning that small changes in the experimental systems lead to small deviations between experimental results and theoretical predictions. As a result, we believe that this ''single molecule'' perspective, which builds on approaches taken to describe the interaction of motor proteins adhered to surfaces with cytoskeletal filaments,[28–30] provides insights complementing more detailed theoretical calculations. The predictions of the RSA model for the dependence of protein adsorption on the model parameters are shown in Figure 5.

Protein adsorption decreases rapidly with an increasing number of ethylene oxide units in the PEO chains (Fig. 5A), because the size of the open space required for adsorption rapidly increases with the increasing height of the polymer chain. However, the residual adsorption for very short chains becomes nearly undetectable (<0.1% of a monolayer) even for moderate grafting ratios. Since the maximum grafting density decreases and the required open space increases with PEO chain length, the possible number of PEO chains in the required open space is maximized at an intermediate chain length. A larger number corresponds to more possibilities to encounter interfering PEO chains and thus reduced protein adsorption.

Unsurprisingly, protein size (Fig. 5B) strongly affects adsorption, suggesting that non-spherical proteins preferentially adsorb in initial orientations that minimize the required open space and that smaller proteins preferentially adsorb from protein mixtures (e.g., serum).

For a given protein size and PEO chain length, PEO chain density (Fig. 5C, D) is a critical parameter displaying a sharp transition between significant adsorption and almost complete resistance to protein adsorption. However, the parameter f, which describes the maximal fraction of the surface covered by protein, can be varied from 1 over 0.9 (representing hexagonal close-packing) and 0.78 (square net) to 0.53 (representing the jamming limit[16,31]) without significantly affecting the predictions at medium and high PEO chain densities (Fig. 5C). Our choice of $f = 0.9$ (hexagonal packing) permits close contact between two adsorbed proteins–a situation which cannot be ruled out at medium to high grafting densities. In contrast, adsorption at low grafting densities is dominated by the obstruction of adsorption by other, already adsorbed proteins–a situation better reflected by $f = 0.53$ (jamming limit).

Similarly, the kinetics of the adsorption process determined by the product of the sticking probability S, the landing rate Z, and the adsorption time t do not have a large effect on the dependence of protein adsorption on PEO chain density (Fig. 5D). Changing the product SZt by an order of magnitude primarily shifts the chain density-dependent transition from the adsorbing to the protein-resistant regime, but by an amount that would be difficult to detect. The adsorption process is predicted to near completion on a timescale of hours, which corresponds to the typically chosen experimental conditions. The time after which the amount of adsorbed protein reaches the detection limit of a typical adsorption measurement (10^{-3} monolayers) increases exponentially with the chain density (see Supporting Information, Fig. S4).

Similar to the demonstrated extension of the model to methyl-terminated PEO chains which facilitate secondary adsorption, random sequential adsorption models can be readily constructed for other classes of surfaces (e.g., the glycocalix), mixed polymer layers, and mixed protein adsorption. Computer simulations promise to answer more detailed questions, for example with respect to the kinetics of the adsorption process near the jamming limit.[15] An application of the RSA model may also benefit a number of newly developed coating system, including ''bottle'' brushes of poly(oligo(ethylene glycol)methyl methacrylate),[32] PEO-grafted poly-(4-benzoyl-p-xylylene-co-p-xylylene) coatings,[33] and plasma-deposited tetraglyme surfaces.[34]

The application of the RSA model may be limited in systems which permit the reorganization of PEO chains into ordered arrangements after the initial adsorption, because the model assumes a random placement. In principle, exchange reactions could lead to such ordering in self-assembled monolayers of alkanethiols, and interactions between PEO chains could drive ordering in physisorbed coatings. However, we believe that the small thermodynamic driving forces, especially at low and medium grafting densities, render such ordering processes exceedingly slow and not important for the experimental systems discussed here.

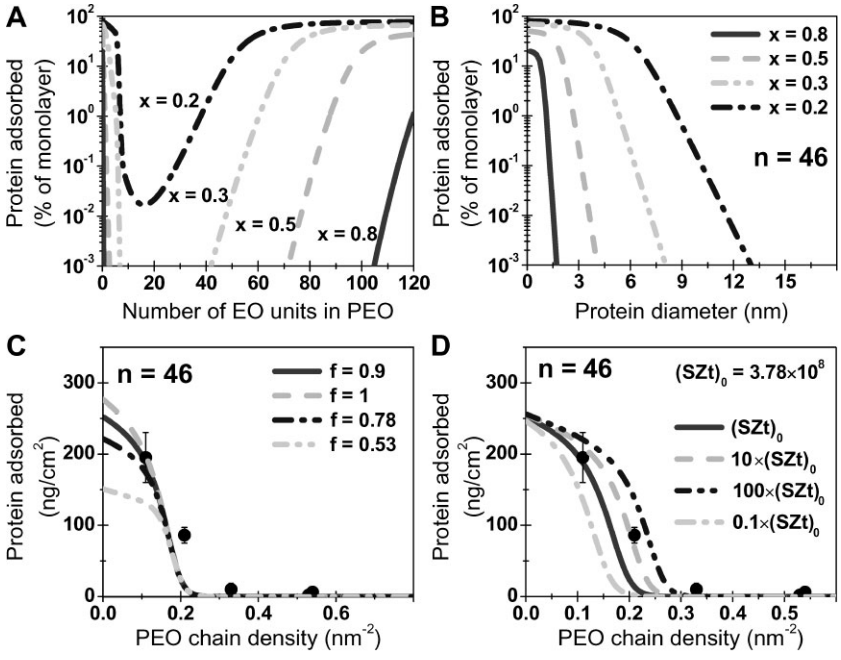

Figure 5. Predictions of the RSA model for primary adsorption. A) Adsorption as function of number of EO units in a PEO chain. B) Adsorption as function of protein diameter for chains with 46 EO units. C) Effect of different values of the parameter f, which describes the maximum possible packing fraction. D) Effect of variations in the product of sticking probability S, landing rate Z, and adsorption time t. The adsorption conditions assumed are those used by Pasche et al. [22] (black circles: experimental data).

The implications of the proposed RSA model for the long-standing debate about the origin of the resistance of PEO-grafted surfaces to protein adsorption are profound. Traditionally, physical (steric exclusion) and chemical (preference for water binding) contributions to the interaction of individual chains with protein and water are juxtaposed.[2] In contrast, the RSA model focuses on the random distribution of the PEO chains on the surface, assuming that the presence of a single PEO chain in the protein–surface contact area completely prevents protein adsorption. The PEO coating thus presents neither a thermodynamic nor a kinetic barrier that is surmounted over time, but a perfect steric barrier with a defined number of holes. The key suggestion for the design of coating procedures is to increase the PEO chain density to reduce residual protein adsorption, which can be detected by single molecule methods.[30] While the need for a full understanding of the enthalpic and entropic interactions between PEO chains, water, and protein cannot be denied,[1,2,35,36] the agreement between the experimental data and the RSA model suggests that the random arrangement of the PEO chains is a major and previously neglected factor in determining protein adsorption to PEO-grafted surfaces.

Acknowledgements

The authors thank Scott Perry for helpful discussions. This work was supported by start-up funds and NSF award DMR-0645023. Supporting Information is available online from Wiley InterScience or from the author.

Received: July 19, 2008
Revised: August 28, 2008
Published online: October 23, 2008

[1] I. Szleifer, *Curr. Opin. Solid State Mater. Sci.* **1997**, *2*, 337.
[2] M. Morra, *J. Biomater. Sci, Polym. Ed.* **2000**, *11*, 547.
[3] R. A. Latour, in *Encyclopedia of Biomaterials and Biomedical Engineering*, (Eds: G. Wnek, G. Bowlin), Taylor&Francis, New York **2005**.
[4] S. I. Jeon, J. H. Lee, J. D. Andrade, P. G. De Gennes, *J. Colloid Interface Sci.* **1991**, *142*, 149.
[5] S. I. Jeon, J. D. Andrade, *J. Colloid Interface Sci.* **1991**, *142*, 159.
[6] I. Szleifer, *Biophys. J.* **1997**, *72*, 595.
[7] J. Satulovsky, M. A. Carignano, I. Szleifer, *Proc. Natl. Acad. Sci. USA* **2000**, *97*, 9037.
[8] M. Agashe, V. Raut, S. J. Stuart, R. A. Latour, *Langmuir* **2005**, *21*, 1103.
[9] J. C. Hower, Y. He, M. T. Bernards, S. Y. Jiang, *J. Chem. Phys.* **2006**, *125*, 214704.
[10] K. L. Prime, G. M. Whitesides, *Science* **1991**, *252*, 1164.
[11] K. L. Prime, G. M. Whitesides, *J. Am. Chem. Soc.* **1993**, *115*, 10714.
[12] J. Gottschalck, B. Hammer, *J. Chem. Phys.* **2002**, *116*, 784.
[13] L. D. Unsworth, H. Sheardown, J. L. Brash, *Langmuir* **2008**, *24*, 1924.
[14] J. W. Evans, *Rev. Mod. Phys.* **1993**, *65*, 1281.
[15] J. Talbot, G. Tarjus, P. R. Van Tassel, P. Viot, *Colloids Surf. A* **2000**, *165*, 287.
[16] J. Feder, *J. Theor. Biol.* **1980**, *87*, 237.
[17] F. Fang, J. Satulovsky, I. Szleifer, *Biophys. J.* **2005**, *89*, 1516.
[18] E. Ostuni, B. A. Grzybowski, M. Mrksich, C. S. Roberts, G. M. Whitesides, *Langmuir* **2003**, *19*, 1861.
[19] K. A. Dill, S. Bromberg, *Molecular Driving Forces*, Taylor and Francis, London **2002**.
[20] D. R. Weaver, W. G. Pitt, *Biomaterials* **1992**, *13*, 577.
[21] L. S. Jung, C. T. Campbell, *Phys. Rev. Lett.* **2000**, *84*, 5164.
[22] S. Pasche, S. M. De Paul, J. Voros, N. D. Spencer, M. Textor, *Langmuir* **2003**, *19*, 9216.
[23] L. E. Ramm, M. B. Whitlow, M. M. Mayer, *J. Immunol.* **1985**, *134*, 2594.
[24] A. Rothen, *J. Gen. Physiol.* **1940**, *24*, 203.
[25] S. Herrwerth, W. Eck, S. Reinhardt, M. Grunze, *J. Am. Chem. Soc.* **2003**, *125*, 9359.
[26] X. L. Wang, P. H. McMurry, *Int. J. Mass Spectrom.* **2006**, *258*, 30.
[27] A. Purice, J. Schou, P. Kingshott, N. Pryds, M. Dinescu, *Appl. Surf. Sci.* **2007**, *253*, 6451.
[28] J. Howard, A. J. Hudspeth, R. D. Vale, *Nature* **1989**, *342*, 154.
[29] W. O. Hancock, J. Howard, *J. Cell Biol.* **1998**, *140*, 1395.
[30] P. Katira, A. Agarwal, T. Fischer, H.-Y. Chen, X. Jiang, J. Lahann, H. Hess, *Adv. Mater.* **2007**, *19*, 3171.
[31] G. Y. Onoda, E. G. Liniger, *Phys. Rev. A* **1986**, *33*, 715.
[32] H. Ma, J. Hyun, P. Stiller, A. Chilkoti, *Adv. Mater.* **2004**, *16*, 338.
[33] H. Y. Chen, J. Lahann, *Anal. Chem.* **2005**, *77*, 6909.
[34] L. Cao, M. Chang, C.-Y. Lee, D. G. Castner, S. Sukavaneshvar, B. D. Ratner, T. A. Horbett, *J. Biomed. Mater. Res. A* **2007**, *81A*, 827.
[35] R. A. Latour, *J. Biomed. Mater. Res. A* **2006**, *78A*, 843.
[36] S. F. Chen, S. Y. Jiang, *Adv. Mater.* **2008**, *20*, 335.